Visibility of Internal Target Volume of Dynamic Tumors in Free-breathing Cone-beam Computed Tomography for Image Guided Radiation Therapy

Kevin I. Kauweloa*[†], Justin C. Park*[†], Ajay Sandhu*, Todd Pawlicki*, Bongyong Song*, William Y. Song*

*Center for Advanced Radiotherapy Technologies and Department of Radiation Medicine and Applied Sciences, University of California San Diego, La Jolla, [†]Department of Physics, San Diego State University, San Diego, [†]Department of Electrical and Computer Engineering, University of California San Diego, La Jolla, CA, USA

Respiratory-induced dynamic tumors render free-breathing cone-beam computed tomography (FBCBCT) images with motion artifacts complicating the task of quantifying the internal target volume (ITV). The purpose of this paper is to study the visibility of the revealed ITV when the imaging dose parameters, such as the kVp and mAs, are varied. The Trilogy[TM] linear accelerator with an On-Board Imaging (OBI[TM]) system was used to acquire low-imaging-dose-mode (LIDM: 110 kVp, 20 mA, 20 ms/frame) and high-imaging-dose-mode (HIDM: 125 kVp, 80 mA, 25 ms/frame) FBCBCT images of a 3-cm diameter sphere (density=0.855 g/cm^3) moving in accordance to various sinusoidal breathing patterns, each with an unique inhalation-to-exhalation (I/E) ratio, amplitude, and period. In terms of image ITV contrast, there was a small overall average change of the ITV contrast when going from HIDM to LIDM of 6.5±5.1% for all breathing patterns. As for the ITV visible volume measurements, there was an insignificant difference between the ITV of both the LIDM- and HIDM-FBCBCT images with an average difference of 0.5±0.5%, for all cases, despite the large difference in the imaging dose (approximately five-fold difference of ~0.8 and 4 cGy/scan). That indicates that the ITV visibility is not very sensitive to changes in imaging dose. However, both of the FBCBCT consistently underestimated the true ITV dimensions by up to 34.8% irrespective of the imaging dose mode due to significant motion artifacts, and thus, this imaging technique is not adequate to accurately visualize the ITV for image guidance. Due to the insignificant impact of imaging dose on ITV visibility, a plausible, alternative strategy would be to acquire more X-ray projections at the LIDM setting to allow 4DCBCT imaging to better define the ITV, and at the same time, maintain a reasonable imaging dose, i.e., comparable to a single HIDM-FBCBCT scan.

Key Words: Internal target volume, Inhalation to exhalation ratio, Imaging dose, Image quality, Free-breathing cone beam computed tomography

INTRODUCTION

In order to optimize respiratory-induced mobile tumors for radiation therapy, the first important step is to image an accurate, representative patient anatomy for planning and treatment delivery. Dynamic tumors can complicate this process.[1-6] However, the advent of four-dimensional computed tomography (4DCT) has significantly alleviated these difficulties by rebinning CT projections to successfully reconstruct images at instantaneous moments/phases, leading to an accurate delineation of the Internal Target Volume (ITV).[1-9] It has been shown by Underberg et al. and Jin et al. that 4DCT images

acquired using respiration-tracking systems can be used for stereotactic body radiotherapy (SBRT) of lung cancer.[8,9]

The integration of the cone-beam computed tomography (CBCT) systems with the clinical linear accelerators has allowed daily assessment of the gross location of the ITV before each treatment, the technique known broadly as image guided radiation therapy (IGRT).[10-16] However, Varian's On Board Imager (OBI[TM]) CBCT system (Varian Medical Systems, Palo Alto, CA), as of this current model, lacks 4DCBCT imaging capability, making accurate assessment of the daily ITV motion range difficult. Resorting to breath-hold and/or free-breathing-3DCBCT techniques are less than ideal since not all patients are breath-hold candidates and that 3DCBCT images can contain significant motion-related artifacts including streaking in axial and blurriness in sagittal/coronal dimensions, respectively.[17-21] Despite the presence of these artifacts, the 3DCBCT images are still relatively useful for gross positioning of dynamic tumors and are in wide clinical use at this time.

Vergalasova et al. investigated motion artifacts, specifically blurring in sagittal/coronal slices, arising from imaging dynamic tumors with varying inhalation-to-exhalation (I/E) ratio (defined as the ratio of the duration of time the patient spends in inhalations versus exhalations during a normal breathing, which is typically < 1), amplitude, and period, using a single 3DCBCT scanning mode (i.e., 100 kVp, 80 mA, and 25 ms/projection).[19] They compared how much of the ITV is revealed using CBCT images acquired with different I/E ratios by calculating the relative pixel-vale difference between the ITV and the background. They showed how the percentage of the ITV revealed changed due to the object's dynamic motion, mainly the I/E ratio parameter, using phantom and patient cases. Their results showed how the percentage of the ITV revealed decreased with the decrease of the I/E ratio due to the smaller amount of projections acquired during the inhalation phase. All of the 3DCBCT images that Vergalasova et al. used were all acquired under the same dose parameters, 100 kVp, 80 mA, and 25 ms/projection.

The theoretical solution to this problem of ITV underestimation caused by low I/E ratios, which most patients have, is to apply 4DCBCT which would create images revealing most of the ITV created by the patient's unique breathing pattern. The main requirement of the application of 4DCBCT

is to acquire sufficient projections during each phase within the breathing pattern to successfully apply the Feldkamp-Davis-Kress (FDK) filtered-back projection (FBP) algorithm. The significant problem with acquiring more projections is the significant increase in exposure to the patient, which in itself, cause more unwanted problems. The ideal solution is to acquire 4DCBCT images without increasing the radiation dose delivered to the patient. Li et al.[22] did a study where they reduced the mA and the gantry rotation speed to acquire a certain amount of projections that would give the patient the same dose as would the typical 3DCBCT scan. They showed that as gantry rotation speed is reduced along with the mA, the relative error of the 4DCBCT images with respect to the 3DCBCT images acquired at a higher dose linearly decreased.

In this study, instead of investigating the impact of the I/E ratio on the revealability of the ITV, as done by Vergalasova et al., we studied the idea of whether decreasing the 3DCBCT scanning dose (reduce kVp and mA) would render significant, quantitative and qualitative differences in the visibility of the ITV that is revealed. Also, instead of lowering the gantry rotation speed and performing 4DCBCT reconstruction like Li et al., we kept the gantry rotation speed constant and just compared 3DCBCT images so the study is specifically focused on the impact of low-dose scanning parameters. This study was done by acquiring high- and low-dose 3DCBCT images under the same breathing parameters (i.e., I/E ratio, amplitude, and period), contouring the ITV using both images, and then comparing the ITV results. This is an important and relevant question today since majority of clinics don't have 4DCBCT capability and that depending on the outcome of the study, it can either help justify or dispute the idea of implementing 4DCBCT imaging with low-dose scanning parameters using current CBCT systems on linacs.[23,24]

MATERIALS AND METHODS

The Varian Trilogy linear accelerator with an OBI[TM] system was used to acquire 3DCBCT images of a QUASAR Multi-Purpose Body Phantom (MODUS, London, Canada). The phantom was placed upon the QUASAR Programmable Respiratory Motion Platform (QPRMP) with a cylindrical cedar wood (density=0.330 g/cc) encapsulating a 3-cm-diameter sphere
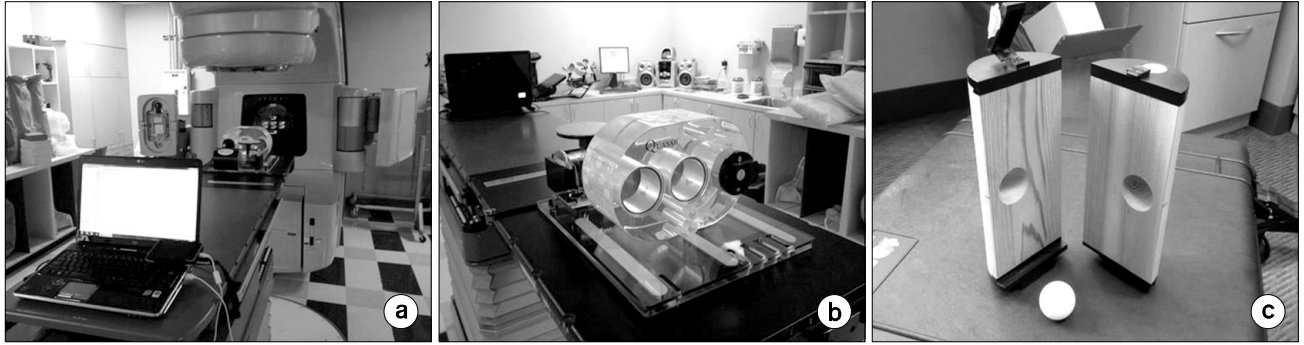
Fig. 1. "Experimental Setup". (a) Front-side view of the setup. (b) Back-side view of the setup with the cylindrical cedar wood containing the sphere placed within the Multi-Purpose Body Phantom. (c) The cylindrical cedar wood and the sphere.

(density=0.855 g/cc) placed within it to mimic lung tissue and solid tumor, respectively. Fig. 1 displays the cylindrical cedar wood, the sphere, and the experimental setup. The QPRMP moved in accordance to thirty different sinusoidal (A$|sin^awt|$) breathing patterns that were made with MATLAB 2010a (Mathworks, Natick, MA). Each sinusoidal pattern differs in parameters such as the I/E ratio, amplitude, and period (Table 1). In this work, the phantom was used to simulate lung cancer patients. Although the densities of the sphere and the surrounding volume were carefully selected to mimic actual patients, we had to confirm/validate our results with a patient case. More patient cases would have made the results more convincing; however, we could not justify the increase in imaging dose for testing on larger cohort of patients.

1. Experiment 1: ITV image contrast

This experiment was designed to study the quantitative differences of the ITV contrast between the low-imaging-dose-mode (LIDM: 110 kVp, 20 mA, 20 ms/frame) and high-imaging-dose-mode (HIDM: 125 kVp, 80 mA, 25 ms/frame) FBCBCT half-fan images, which is approximately five-fold increase in imaging dose (~0.8 and 4 cGy/scan, respectively) and encompasses most of the imaging dose range encountered in clinics.[22] The QPRMP was set to move in accordance to thirty different sinusoidal breathing patterns, each with a distinct set of parameters: amplitude=1 and 3 cm, period=2, 4, and 6 seconds, and I/E ratio=0.2131 to 1, as are shown in Table 1. Each breathing pattern was scanned twice, the first being the LIDM and the second being the HIDM.

Table 1. Percent differences in ITV-contrast between LIDM and HIDM FBCBCT images.

	ITV contrast percent difference			
Wave #	Amplitude (cm)	Period (sec)	I/E ratio	Percent diff (%)
1	1	2	1.0000	2.8
2	1	2	0.5349	2.8
3	1	2	0.3725	−1.4
4	1	2	0.2632	3.7
5	1	2	0.2131	10.1
6	1	4	1.0000	7.1
7	1	4	0.5349	6.8
8	1	4	0.3725	3.2
9	1	4	0.2632	6.8
10	1	4	0.2131	6.2
11	1	6	1.0000	12.1
12	1	6	0.5349	10.8
13	1	6	0.3725	6.1
14	1	6	0.2632	9.1
15	1	6	0.2131	6.1
16	3	2	1.0000	11.3
17	3	2	0.5349	10.3
18	3	2	0.3725	7.5
19	3	2	0.2632	8.1
20	3	2	0.2131	4.6
21	3	4	1.0000	13.5
22	3	4	0.5349	14.1
23	3	4	0.3725	13.7
24	3	4	0.2632	11.1
25	3	4	0.2131	10.8
26	3	6	1.0000	3.6
27	3	6	0.5349	−4.1
28	3	6	0.3725	1.6
29	3	6	0.2632	3.8
30	3	6	0.2131	−7.3
		AVG	0.4767	6.50
		SD	0.2888	5.13

A common image metric used to determine the quality of an image is the contrast to noise ratio (CNR) but we feel that it is not applicable in this study due to its circumstantial inaccuracy. For example, streak artifacts may reduce the average pixel value within the background, in result, increasing the CNR. Instead of using CNR, we will use the ITV-contrast which will quantify the relative signal of the revealed ITV with respect to the background. The ITV-contrast is,

$$C_{ITV} = \frac{I_T - I_b}{I_b} \qquad (1)$$

The average pixel value of each row within the five center-profiles of the coronal slice image is defined as the Target Value I_T, and the average CT number of four 10×10 (pixels) regions-of-interest (ROI) surrounding the sphere's ITV is defined as the background pixel value I_b.

Fig. 2 pictorially explains how I_b and I_T is calculated. The final profile is filled with the ITV-contrast value for each row from top to bottom of the coronal slice image. The average ITV-contrast is calculated by using all ITV-contrast values within the final profile. Once that is completed for the LIDM and HIDM images, the percentage change of the average ITV-contrast value from HIDM to LIDM is calculated with:

$$Percent\ Change = \frac{\overline{C_{ITV-LIDM}} - \overline{C_{ITV-HIDM}}}{\overline{C_{ITV-HIDM}}} \times 100\% \qquad (2)$$

Table 1 lists the percent change for each of the thirty different sinusoidal breathing patterns used in this experiment. In the percent change column, the '+' and '−' signs indicate whether the LIDM average ITV-contrast was 'lesser' or 'greater' than the HIDM average ITV-contrast, respectively.

2. Experiment 2: Revealed ITV

This experiment uses the same simulated breathing patterns that were used in Experiment 1. Using the contouring tools of software ImageJ[TM] (National Institutes of Health, USA), the distance from the top to the bottom of the ITV within both the LIDM and HIDM sagittal and coronal 3DCBCT images are manually measured so the visual ITV size can be calculated. Also calculated is the ground-truth ITV size by using the diameter of the sphere and the amplitude of the breathing pattern. For amplitudes 1 and 3 cm, the volumes were 21.21 cm^3 and 35.34 cm^3, respectively.

The visible and ground-truth ITV are used to make two important calculations: 1) the percent difference between the visible ITV and ground-truth ITV and 2) the percent difference between the two visible ITVs between the two LIDM and HIDM imaging modes. The Equation that was used to calculate the percent difference is:
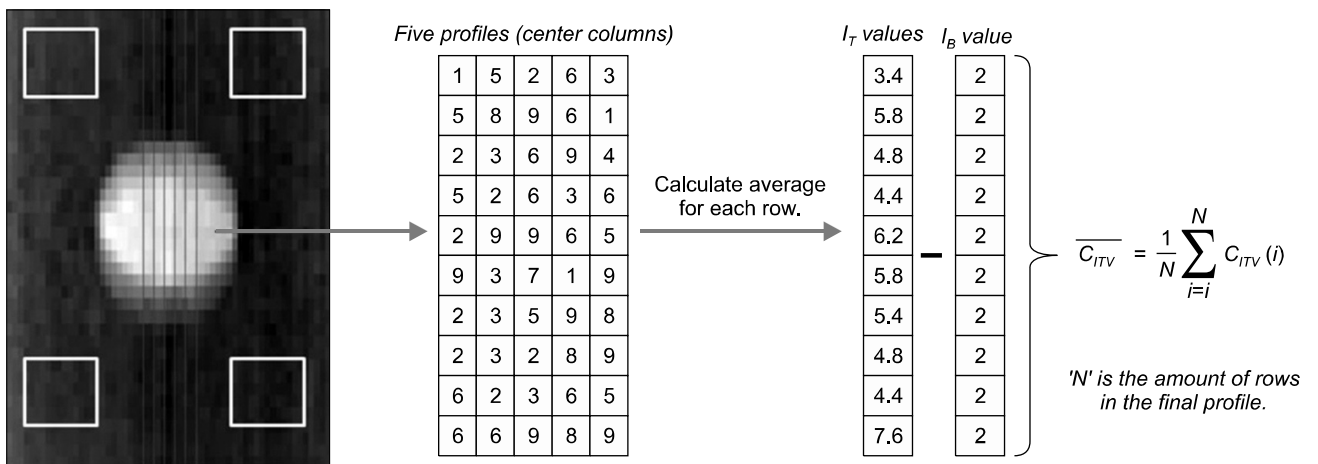

Fig. 2. "ITV Contrast Calculation". An illustration of how the ITV contrast is calculated using an example coronal image slice of a FBCBCT scan. The four yellow squares represent the 10×10-pixels ROIs that were used to calculate the I_b. The average pixel values of the five central colums of the ITV were used to calculate the the I_T.
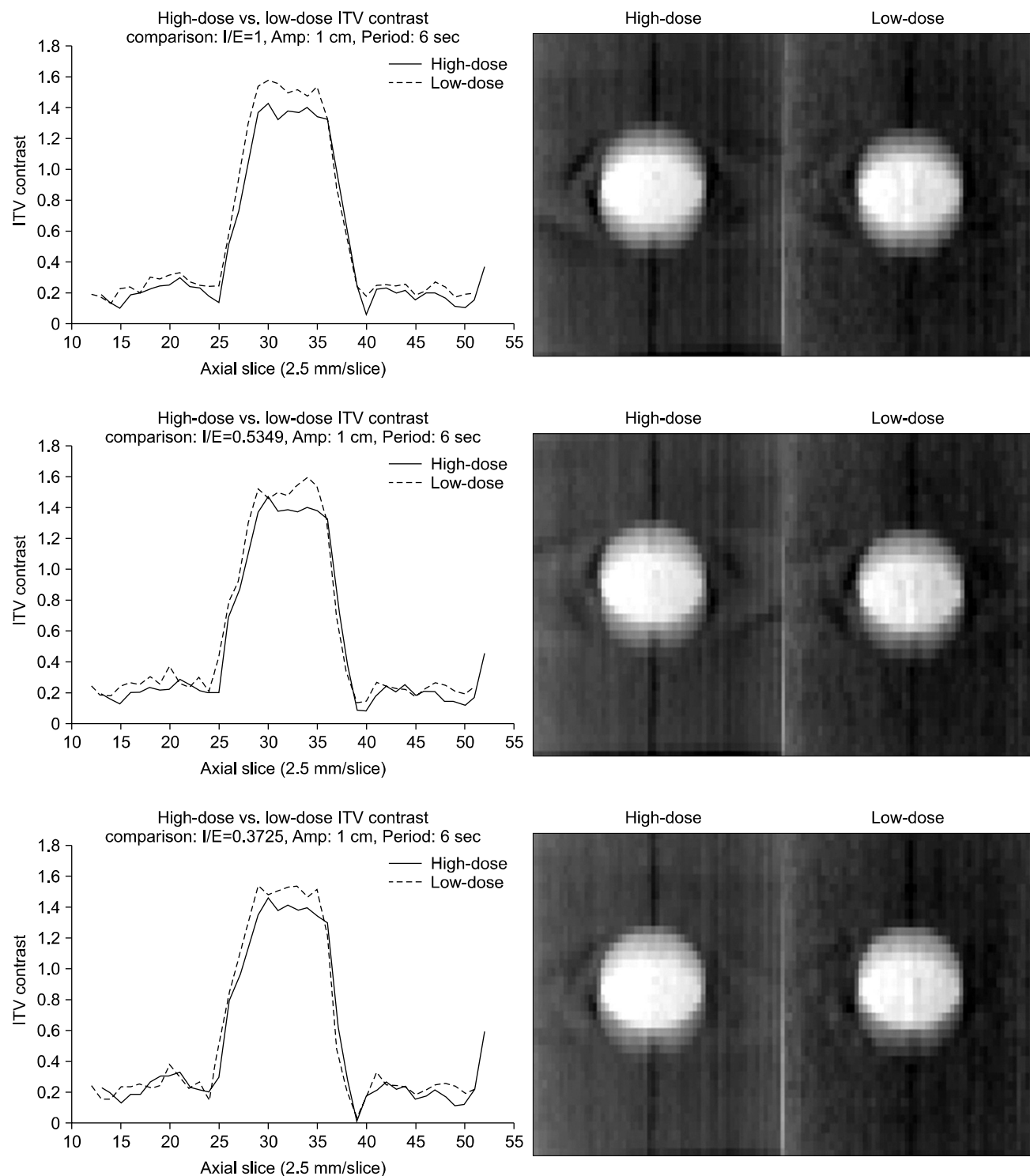
Fig. 3. "Central Profile Comparison". An example case showing the central profiles of the LIDM and HIDM FBCBCT images with I/E ratios ranging from 0.2632 through 1, amplitude=1 cm, and period=6 seconds.
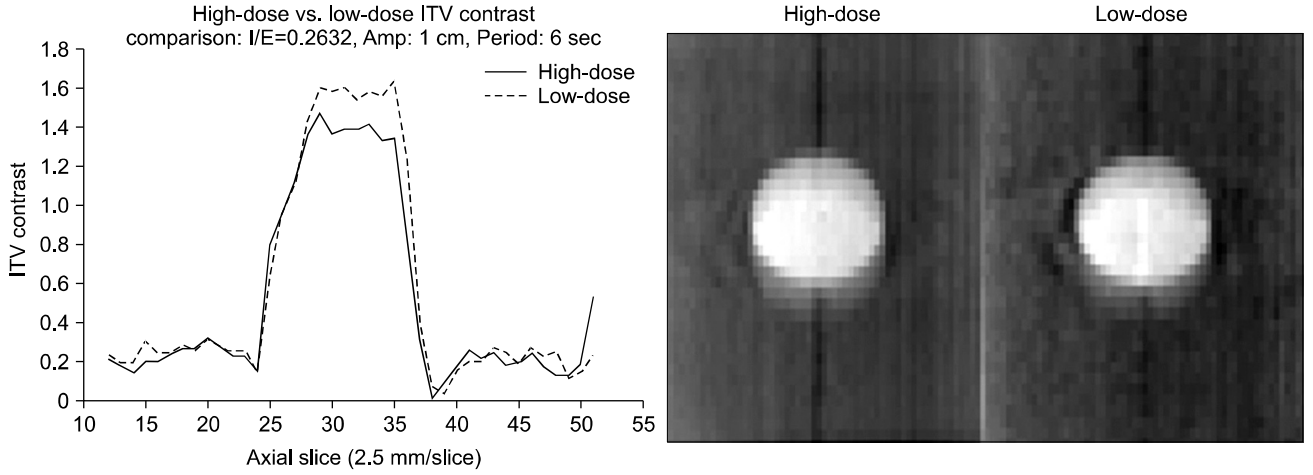
High-dose vs. low-dose ITV contrast comparison: I/E=0.2632, Amp: 1 cm, Period: 6 sec

Fig. 3. Continued.

$$PD = \frac{|ITV_{visible} - ITV_{ground-truth}|}{ITV_{ground-truth}} \times 100\% \qquad (3)$$

The equation that was used to calculate the percent difference between the two visible ITVs is:

$$PD = \frac{|ITV_{LIDM} - ITV_{HIMD}|}{ITV_{HIDM}} \times 100\% \qquad (4)$$

In addition to the thirty simulated breathing patterns, one clinical patient was scanned consecutively with the LIDM and HIDM 3DCBCT protocols in a single treatment session to validate the results obtained with the phantom measurements.

RESULTS

1. Experiment 1: ITV image contrast

Table 1 lists the percent change in ITV-contrast from HIDM to LIDM 3DCBCT images. The percent changes were generally independent of the amplitude, period, and/or I/E ratio. In addition, the overall percent change was 6.5±5.1% indicating a very small increase with the low imaging dose, but clinically insignificant difference in the ITV contrast between the two images. Fig. 3 shows a sample case for an amplitude of 1 cm.

2. Experiment 2: Revealed ITV

Tables 2 and 3 list the percent differences between the two revealed and ground-truth ITVs for amplitudes of 1 and 3 cm, respectively. The percent changes were generally independent of the period. However, the I/E ratio was an important factor in the difference between the revealed and the ground-truth ITV sizes, as the difference increased when the I/E ratio decreased. The most significant ITV underestimations were observed when the I/E ratio was small and the amplitude was large. When the amplitude was 1 cm, the percent difference did not exceed 12%, but when amplitude increased to 3 cm, this increased to >34%.

Despite the large ITV underestimations compared with the ground-truth, the percent difference between the two revealed ITVs of the LIDM and HIDM 3DCBCT images was consistently insignificant as shown in Fig. 4. For an amplitude of 1 cm, the overall percent difference was 0.2±0.2%, and for an amplitude of 3 cm, it was 0.8±0.5%. The overall difference was 0.5±0.5%, which is consistent with the ITV-contrast analysis results in Experiment 1, suggesting that the image quality for visualizing the ITV is generally equal between the two imaging dose modes, which further suggests that increasing the imaging dose (up to ~4 cGy/scan) is not necessarily beneficial.

Fig. 5 displays few example cases of the images. As can be seen, the visual difference in the image quality between the two imaging modes is quite small. Fig. 6 shows the patient case. It can be seen that the image quality between the two imaging modes are similar, in terms of ITV visualization, confirming the phantom results. A Radiation Oncologist was

Table 2. Percent changes in the visual ITVs and the ground-truth for cases with amplitude of 1 cm.

| Volumetric percent difference (PD) between: 1. HIDM/LIDM & true volume 2. LIDM & HIDM | | | | |
Amp., period, I/E ratio	Imaging mode	Measured ITV (cm^3)	PD from ground-truth (%)	PD between LIDM and HIDM (%)
1 cm, 2 sec, I/E=1.0000	HIDM	19.91	−6.1	0.33
	LIDM	19.98	−5.8	
1 cm, 2 sec, I/E=0.5349	HIDM	19.53	−7.9	0.04
	LIDM	19.53	−7.9	
1 cm, 2 sec, I/E=0.3725	HIDM	19.53	−7.9	0.01
	LIDM	19.53	−7.9	
1 cm, 2 sec, I/E=0.2632	HIDM	18.76	−11.6	0.16
	LIDM	18.79	−11.4	
1 cm, 2 sec, I/E=0.2131	HIDM	18.79	−11.4	0.18
	LIDM	18.82	−11.3	
1 cm, 4 sec, I/E=1.0000	HIDM	19.94	−6.0	0.01
	LIDM	19.94	−6.0	
1 cm, 4 sec, I/E=0.5349	HIDM	19.53	−7.9	0.01
	LIDM	19.53	−7.9	
1 cm, 4 sec, I/E=0.3725	HIDM	19.56	−7.8	0.12
	LIDM	19.53	−7.9	
1 cm, 4 sec, I/E=0.2632	HIDM	18.79	−11.4	0.15
	LIDM	18.81	−11.3	
1 cm, 4 sec, I/E=0.2131	HIDM	18.85	−11.1	0.51
	LIDM	18.76	−11.6	
1 cm, 6 sec, I/E=1.0000	HIDM	20.10	−5.2	0.63
	LIDM	19.98	−5.8	
1 cm, 6 sec, I/E=0.5349	HIDM	19.59	−7.6	0.33
	LIDM	19.53	−7.9	
1 cm, 6 sec, I/E=0.3725	HIDM	19.62	−7.5	0.33
	LIDM	19.56	−7.8	
1 cm, 6 sec, I/E=0.2632	HIDM	18.79	−11.4	0.04
	LIDM	18.78	−11.5	
1 cm, 6 sec, I/E=0.2131	HIDM	18.83	−11.2	0.39
	LIDM	18.76	−11.6	

Table 3. Percent changes in the visual ITVs and the ground-truth for cases with amplitude of 3 cm.

Amp., period, I/E ratio	Imaging mode	Measured ITV (cm^3)	PD from ground-truth (%)	PD between LIDM and HIDM (%)
3 cm, 2 sec, I/E=1.0000	HIDM	31.90	−9.7	0.19
	LIDM	31.84	−9.9	
3 cm, 2 sec, I/E=0.5349	HIDM	31.39	−11.2	1.03
	LIDM	31.07	−12.1	
3 cm, 2 sec, I/E=0.3725	HIDM	31.13	−11.9	0.82
	LIDM	30.88	−12.6	
3 cm, 2 sec, I/E=0.2632	HIDM	23.57	−33.3	1.63
	LIDM	23.18	−34.4	
3 cm, 2 sec, I/E=0.2131	HIDM	23.50	−33.5	1.93
	LIDM	23.05	−34.8	
3 cm, 4 sec, I/E=1.0000	HIDM	32.22	−8.8	0.19
	LIDM	32.16	−9.0	
3 cm, 4 sec, I/E=0.5349	HIDM	31.84	−9.9	1.21
	LIDM	31.46	−11.0	
3 cm, 4 sec, I/E=0.3725	HIDM	31.47	−11.9	0.25
	LIDM	31.07	−12.1	
3 cm, 4 sec, I/E=0.2632	HIDM	24.24	−31.4	0.41
	LIDM	24.14	−31.7	
3 cm, 4 sec, I/E=0.2131	HIDM	23.80	−32.6	0.81
	LIDM	23.61	−33.2	
3 cm, 6 sec, I/E=1.0000	HIDM	31.84	−9.9	0.75
	LIDM	32.08	−9.2	
3 cm, 6 sec, I/E=0.5349	HIDM	31.46	−11.0	1.52
	LIDM	30.98	−12.3	
3 cm, 6 sec, I/E=0.3725	HIDM	31.07	−12.1	0.45
	LIDM	30.93	−12.5	
3 cm, 6 sec, I/E=0.2632	HIDM	23.86	−32.5	0.61
	LIDM	22.71	−32.9	
3 cm, 6 sec, I/E=0.2131	HIDM	23.82	−32.6	0.65
	LIDM	23.66	−33.0	

asked to contour the visible ITVs of the two images, the results of which was consistent with the volume difference of 1.8% (ITV=19.62 vs 19.98 cm^3).

DISCUSSION

It is well known that increasing the imaging dose improves image quality by improving contrast and resolution, yet even with high-dose scanning parameters, motion artifacts such as blurring are still present. As the kVp and mA are lowered, a reduction in photon flux will increase the noise[25,26] but since the motion artifacts are still present, the purpose of this paper was to investigate the impact of the target's dynamic properties on the ITV visibility explicitly due to the noise.

Our results display the insignificant impact of the additional noise when contouring ITVs using low-dose 3DCBCT images. When comparing the ITV calculations using both LIDM and HIDM 3DCBCT images, the differences were small. For breathing patterns with an amplitude of 1 cm, the overall percent was 0.2±0.2%, and for amplitude=3 cm, it was 0.8±0.5%. Overall, the difference was 0.5±0.5%. This shows that if the dose is reduced and the gantry rotation speed remains constant, the ITV will be sufficiently visible to produce accurate approximations of the ITV that would be acquired from high-
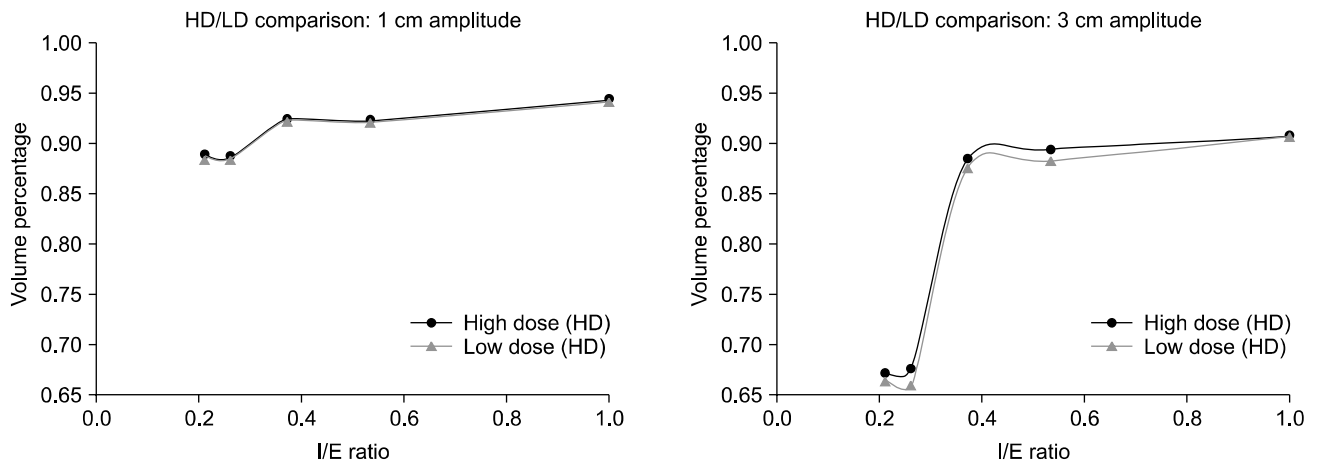
Fig. 4. "HD_LD Comparison". As seen for both amplitudes, the accuracy of volume measurement worsens as the I/E ratio decreases. Despite that, the difference in volume measurement with HIDM and LIDM FBCBCTs is insignificant.
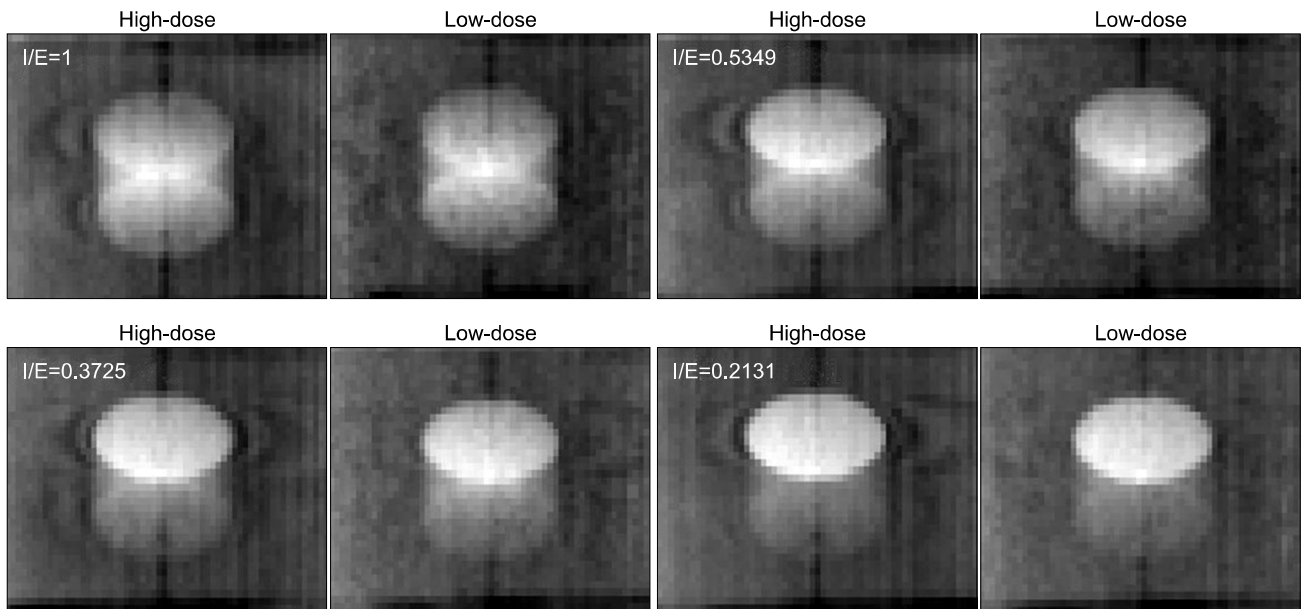

Fig. 5. "I/E Ratio HD_LD Comparisons". Representative cases of the LIDM and HIDM FBCBCT images illustrating the similarity in ITV visibility between two modes.

dose 3DCBCT images. This also further supports the work done by Li et al., where their results suggested that the difference between low-dose 4DCBCT images is insignificant when compared to 3DCBCT images acquired with the dose scanning parameters set to 80 mA and 125 kVp which was considered the "gold standard" in their study.

With the I/E ratios less than 1, 3DCBCT images consistently underestimated the true ITV dimensions by up to 34.8%

irrespective of the imaging dose mode due to significant motion artifacts, and thus, this imaging technique is not adequate to accurately calculate the true ITV for image guidance. Due to the insignificant impact of imaging dose on ITV visibility in this study as well as in the work by Li et al., a plausible alternative strategy would be to acquire more CBCT projections at the LIDM setting to allow 4DCBCT imaging to better define the ITV, and at the same time, maintain a reasonable
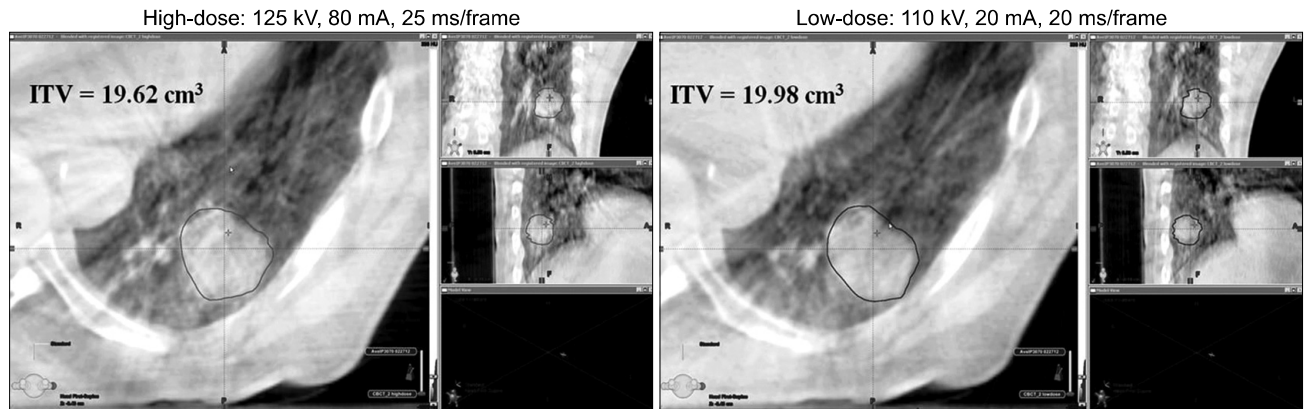
High-dose: 125 kV, 80 mA, 25 ms/frame

Low-dose: 110 kV, 20 mA, 20 ms/frame

Fig. 6. "HD_LD Contour Comparison". A representative, example patient case imaged with both the LIDM and HIDM FBCBCTs. An expert Radiation Oncologist contoured the visible ITVs on each image.

imaging dose, i.e., comparable to a single HIDM-3DCBCT scan.

Despite the positive results with the use of low-dose 3DCBCT images, as well as those of low-dose 4DCBCT images as shown by Li et al., one problem still needs to be addressed which is the extension of time necessary to acquire more projections with low-dose scanning parameters to apply 4DCBCT. The limitation of the amount of low-dose CBCT projections acquired for 4DCBCT is set by the goal of not giving the patient more dose than he/she would receive if given a typical 3DCBCT scan. In order to acquire the maximum amount of low-dose CBCT projections, more time will be needed than the time needed to apply 3DCBCT. That raises the probability of acquiring worthless projections due to the patient moving during the scan. If this problem can be solved, applying 4DCBCT with low-dose scanning parameters and using the FDK reconstruction technique is supported to be a viable, clinical idea.

CONCLUSION

Our study confirmed and showed that the significance of the ITV underestimation is inversely proportional to the I/E ratio which renders the idea of applying low-dose 4DCBCT imaging viable and important. Our study also showed that when more noise is present in images when using low-dose scanning parameters (LIDM: 110 kVp, 20 mA, 20 ms/frame) under ideal circumstances of the size and location of the target (e.g., tu-

mor in lung of large air pockets), the visibility of the revealed ITV was insignificantly impacted when compared to HIDM 3DCBCT images acquired with the same breathing parameters (e.g., I/E ratio, amplitude, and period). This study lays the foundation for more investigation of low-dose 4DCBCT for dynamic tumors such as studying different target sizes, locations, minimum dose scanning parameters, etc.

REFERENCES

1. **Vedam SS, Keall PJ, Kini VR, et al**: Acquiring a four-dimensional computed tomography dataset using an external respiratory signal. Phys Med Biol 48(1):45–62 (2003)
2. **Lu W, Parikh PJ, Hubenschmidt JP, et al**: A comparison between amplitude sorting and phase angle sorting using external respiratory measurement for 4DCT. Med Phys 33(8):2964–2974 (2006)
3. **Keall PJ**: 4-Dimensional computed tomography imaging and treatment planning. Semin Radiat Oncol 14(1):81–90 (2004)
4. **Low DA, Nystrom M, Kalinin F, et al**: A method for the reconstruction of four-dimensional synchronized CT scans acquired during free breathing. Med Phys 30(6):1254–1263 (2003)
5. **Fitzpatrick MJ, Starkschall G, Antolak JA**: Displacement-based binning of time-dependent computed tomography image data sets. Med Phys 33(1):235–246 (2006).
6. **Wink NM, Panknin C, Soldberg TD**: Phase versus amplitude sorting of 4D-CT data. J Appl Clin Med Phys 7(1):77–85 (2006)
7. **Ruan D, Fessler JA, Balter JM**: Mean position tracking of respiratory motion. Med Phys 35(2):782–792 (2008)
8. **Underberg RW, Lagerwaard FJ, Cuijpers JP, et al**: Four-dimensional CT scans for treatment planning in stereotactic radiotherapy for stage I lung cancer. Int J Radiat Oncol Biol Phys

60:1283-1290 (2004)

9. Jin JY, Ajlouni M, Chen Q, et al: A technique of using gated-CT images to determine internal target volume (ITV) for fractionated stereotactic lung radiotherapy. Radiother Oncol 78: 177-184 (2006)

10. Purdie TG, Bissonnette JP, Franks K, et al: Cone-beam computed tomography for on-line image guidance of lung stereotactic radiotherapy: Localization, verification, and intrafraction tumor position. Int J Radiat Oncol Biol Phys 68(1):243-252 (2007)

11. Yeung AR, Li JG, Shi W, et al: Tumor localization using cone-beam CT reduces setup margins in conventionally fractionated radiotherapy for lung tumors. Int J Radiat Oncol Biol Phys 74(4):1100-1107 (2009)

12. Grills IS, Hugo G, Kestin LL, et al: Image-guided radiotherapy via daily online cone-beam CT substantially reduces margin requirements for stereotactic lung radiotherapy. Int J Radiat Oncol Biol Phys 70(4):1045-1056 (2008)

13. Yin FF, Wang Z, Yoo S, et al: Integration of cone-beam CT in stereotactic body radiation therapy. Technol Cancer Res Treat 7(2):133-139 (2008)

14. Yin FF, Wang Z, Yoo S, et al: In-room radiographic imaging for localization. Proceedings AAPM Summer School Integrating New Technologies into the Clinic: Monte Carlo and Image Guided Radiation Therapy. 2006, Ontario, Canada

15. Thilmann C, Nill S, Tucking T, et al: Correction of patient positioning errors based on in-line cone beam CTs: clinical implementation and first experiences. Radiother Oncol 1:16 (2006)

16. Li T, Schreibmann E, Yang Y, et al: Motion correction for improved target localization with on-board cone-beam computed tomography. Phys Med Biol 51:253-267 (2006)

17. Duggan DM, Ding GX, Coffey CW, et al: Deep-inspiration breath-hold kilovoltage cone-beam CT for setup of stereotactic body radiation therapy for lung tumors: Initial experience. Lung Cancer 56(1):77-88 (2007)

18. Yin FF, Das S, Kirkpatrick J, et al: Physics and imaging for targeting of oligometastases. Semin Radiat Oncol 16(2):85-101 (2006)

19. Vergalasova I, Maurer J, Yin FF: Potential underestimation of the internal target volume (ITV) from free-breathing CBCT. Med Phys 38(8):4689-4699 (2011)

20. Buzug TM: Computed Tomography: From Photon Statistics to Modern Cone-Beam CT. 1st ed, Springer-Verlag Berlin, Heidelberg (2008) pp. 521

21. Hsieh J: Computed Tomography: Principles, Design, Artifacts, and Recent Advances. 2nd ed, SPIE/John Wiley & Songs, Inc. (2009) pp. 556

22. Li T, Xing L: Optimizing 4D cone-beam CT acquisition protocol for external beam radiotherapy. Int J Radiat Oncol Biol Phys 67(4):1211-1219 (2007)

23. Song WY, Kamath S, Ozawa S, et al: A dose comparison study between XVI and OBI CBCT systems. Med Phys 35(2): 480-486 (2008)

24. Sonke JJ, Zijp L, Remeijer P, et al: Respiratory correlated cone beam CT. Med Phys 32(4):1176-1186 (2005)

25. Nakayama Y, Awai K, Funama Y, et al: Abdominal CT with low Tube Voltage: Preliminary Observations about Radiation Dose, Contrast Enhancement, Image Quality, and Noise. Radiology 237(3):945-951 (2005)

26. Hsieh J: Adaptive streak artifact reduction in computed tomography resulting from excessive x-ray photon noise. Med Phys 25(11):2139-2147 (1998)